Human Molecular Genetics, 2003, Vol. 12, No. 20 **2703–2710**
DOI: 10.1093/hmg/ddg274

Cellular and subcellular localization of the ARPKD protein; fibrocystin is expressed on primary cilia

Christopher J. Ward[1], David Yuan[1], Tatyana V. Masyuk[2], Xiaofang Wang[1], Rachaneekorn Punyashthiti[1], Shelly Whelan[1], Robert Bacallao[3], Roser Torra[4], Nicholas F. LaRusso[2], Vicente E. Torres[1] and Peter C. Harris[1,*]

[1]Division of Nephrology and [2]Division of Gastroenterology and Hepatology, Mayo Clinic, Rochester, MN, USA, [3]Department of Medicine, Indiana University Medical Center, Indianapolis, IN, USA and [4]Department of Nephrology, Fundació Puigvert, Barcelona, Spain

Received July 9, 2003; Revised and Accepted August 5, 2003

Autosomal recessive polycystic kidney disease (ARPKD) is an infantile form of PKD characterized by fusiform dilation of collecting ducts and congenital hepatic fibrosis. The ARPKD gene, *PKHD1*, is large (~470 kb; 67 exons) with a 12 222 bp longest open reading frame, although multiple different splice forms may be generated. The predicted full-length ARPKD protein, fibrocystin, is membrane bound with 4074 amino acids (447 kDa molecular weight). To characterize the pattern of fibrocystin expression we have generated four monoclonal antibodies (mAb) to the cytoplasmic tail of the protein. Western analysis of human kidney membrane protein showed an identical pattern with each mAb; a strongly expressing large product (>450 kDa), consistent with the predicted protein size, and a weaker ~220 kDa band. The same large product was detected in rat and mouse kidney with lower level expression in liver. To further show that these mAbs recognize fibrocystin, tissue from ARPKD patients was analyzed and no fibrocystin products were detected. Immunohistochemical analysis of the developing kidney showed expression in the branching ureteric bud and collecting ducts, expression that persisted into adulthood. Biliary duct staining was found in the liver, plus staining in the pancreas and developing testis. Immunofluorescence analysis of MDCK cells showed a major site of expression in the primary cilia. Recent studies have associated the disease protein in various human and animal forms of PKD with cilia. The localization of fibrocystin to cilia further strengthens that correlation and indicates that the primary defect in ARPKD may be linked to ciliary dysfunction.

INTRODUCTION

The polycystic kidney diseases (PKD) are a group of inherited disorders characterized by defects in renal tubular maturation, resulting in dilated tubules and/or focal cyst development. The different forms of PKD have related features, including cellular de-differentiation, polarization abnormalities and extracellular matrix remodeling, but it is unclear whether these result from disruption of a common pathogenic pathway (1,2). Several animal models of PKD have revealed a connection to primary cilia. The protein defective in the *orpk* mouse, polaris, is orthologous to the *Chlamydomonas* intraflagellar transport (IFT) protein IFT88 (3). Mice null for this gene (*Tg737*) have left–right axis defects, due to loss of nodal cilia, and the hypomorphic mutant, $Tg737^{orpk}$, has shorted cilia (3,4). The *inv* model of PKD has situs inversus and, like the *orpk* and *cpk* models, the defective protein is located on cilia (5–9). Furthermore, a conditional knockout that disrupts a ciliary motor subunit gene, *Kif3a*, in collecting ducts, lacks cilia and develops cysts (10). Recently, the autosomal dominant PKD (ADPKD) proteins, polycystin-1 and -2, have been localized to cilia; *Pkd2* null animals exhibit left–right axis defects and *Pkd1* null cells lack the flow response usually mediated by cilia (11–15). Therefore, many forms of PKD are associated with defects in ciliary expressed proteins, suggesting a causative role for this organelle in PKD.

Autosomal recessive polycystic kidney disease (ARPKD) is an inherited infantile form of PKD with an incidence of ~1/20 000 (16,17). The typical disease presentation is of greatly enlarged kidneys detected *in utero* or in the perinatal period, with 30% of cases dying shortly after birth (18,19). The massive kidneys are characterized by fusiform dilation of collecting ducts, although

*To whom correspondence should be addressed at: 760 Stabile Building, Mayo Clinic, 200 First Street SW, Rochester, MN 55905, USA. Tel: +1 5072660541; Fax: +1 5072669315; Email: harris.peter@mayo.edu

kidney enlargement is less marked and cyst size more variable in later presenting cases (20,21). The other pathognomonic lesion in ARPKD is biliary dysgenesis, manifesting as dilation of the intrahepatic bile ducts (Caroli's disease) and/or congenital hepatic fibrosis, which is often the major disease complication in older patients (22).

The ARPKD gene, *PKHD1*, was linked to chromosome region 6p21-cen in 1994 and recently identified by characterization of an orthologous rat model, PCK, and by positional cloning (23–25). *PKHD1* is an exceptionally large gene (~470 kb; 67 exons) with a longest open reading frame of 12 222 bp (24). Expression analysis suggests that multiple different splice forms are generated by *PKHD1*, and the murine ortholog, *Pkhd1* (24–27). The gene is strongly expressed in adult and fetal kidney with lower levels in liver, pancreas and lung (24,25). Other specific sites of expression, some of particular splice forms, have been suggested by *in situ* hybridization in the mouse (26).

The ARPKD protein, fibrocystin, is predicted to have 4074 amino acids (4059 amino acids in the mouse) with a calculated unglycosylated molecular weight of 447 kDa (24,25). However, the mature protein may be significantly larger as there are multiple potential N-linked glycosylation sites. Fibrocystin has a signal peptide, and structural predictions indicate a large extracellular region with multiple copies of the TIG domain (an immunoglobulin-like fold), a single transmembrane region, and a short cytoplasmic tail (24,28). A homologous gene, not involved in renal cystic disease, *PKHDL1*, has recently been described (29). The role of other TIG containing proteins, such as the hepatocyte growth factor receptor (Met) and the plexins, and the structure of fibrocystin, suggest that it may be a receptor protein (24,30,31). However, secreted forms of fibrocystin may also be generated from alternatively spliced transcripts (24,25,27).

To characterize the cellular and subcellular distribution of fibrocystin, we raised monoclonal antibodies (mAb) to the C-terminal tail of the protein. Analysis by western blotting, immunohistochemistry, and immunofluorescence have characterized the expression of this protein and showed that fibrocystin is also a ciliary protein.

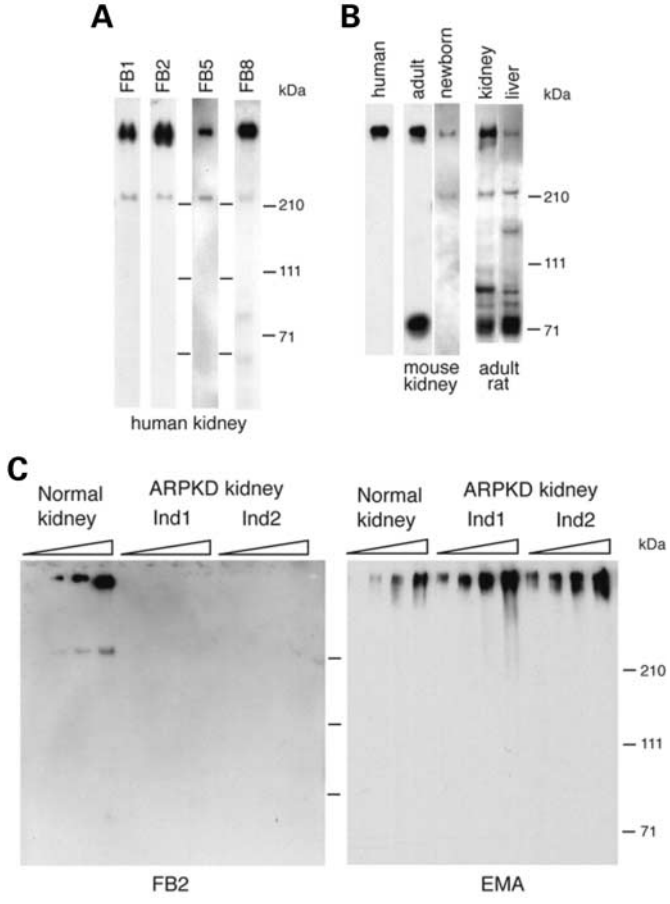

Figure 1. Western analysis of membrane protein separated on 3–8% gradient gels and detected with fibrocystin antibodies. (**A**) Human kidney protein (6–9 μg) shows the same expression pattern with four different fibrocystin mAbs, FB1, FB2, FB5, and FB8. (**B**) The same large (>450 kDa) product is detected in human, mouse, and rat kidney protein (6–12 μg) and newborn mouse kidney (5 μg). The >450 kDa and ~220 kDa products, plus a ~150 kDa protein, were detected in rat liver membrane protein (12 μg). Human and mouse kidney was detected with FB1 and other samples with FB2. Immunoglobulin products (~70–100 kDa) are detected with the secondary antibody in the adult rodent tissue. (**C**) ARPKD and normal kidney protein (0.75, 1.5, 3 and 6 μg) detected with FB2 and EMA. No fibrocystin products are detected in the disease kidney tissue.

RESULTS

Western analysis of normal and ARPKD kidney

A 576 bp fragment of *PKHD1* (11 647–12 222 nt), encoding the entire predicted 192 amino acids cytoplasmic tail of fibrocystin, was amplified by PCR and cloned into a modified pET-43a+ vector to generate recombinant protein (see Methods for details). The purified fibrocystin fragment (~24 kDa) was used to raise mAbs in mice and 500 clones were tested for specificity. Clones were initially screened by an ELISA assay against the purified fibrocystin fragment and positives tested for western detection of recombinant protein and staining of human kidney. Four clones (FB1, FB2, FB5 and FB8), positive in all assays, were selected and are described in this study.

To characterize the endogenous fibrocystin, western blots of human kidney membrane protein were probed with each of the mAb clones. A large, strongly expressing product was detected in each case, plus a weaker ~220 kDa protein (Fig. 1A). The large product (and sometimes the smaller one) was also detected in renal membrane protein isolated from adult mouse and rat; similar results were obtained with newborn kidney tissue (Fig. 1B). To determine the approximate size of the large product (that was significantly larger than those in the marker), the blot was redetected with a murine utrophin mAb that identifies a ~400 kDa product (32). The fibrocystin product was slightly larger, allowing a size estimation of >450 kDa. This size is consistent with the predicted full-length size of fibrocystin.

To further confirm that these mAbs detect fibrocystin, a western blot of normal and ARPKD kidney membrane tissue was prepared. The tissue was isolated from three patients shown to have *PKHD1* mutations: Ind1 (W3871X and E1995G), Ind2 (10627delT and I2957T) and L3 [T36M and

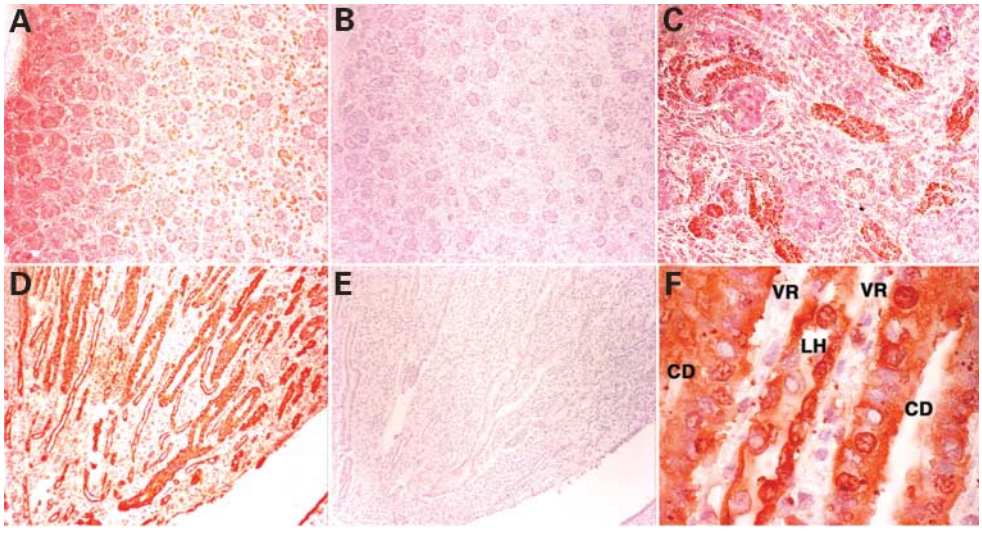

Figure 2. Immunohistochemical staining for fibrocystin in 26-week-old fetal (**A**–**C**) and 4-month-old (**D**–**F**) kidneys, using the FB1 monoclonal antibody. In the fetal kidney the branching ureteric bud (C) and collecting ducts stain strongly; weak immunostaining can also be detected in elongating nephrons. In the 4 month old kidney, the collecting ducts (CD) stain strongly; positive staining can also be detected in the loops of Henle (LH), but not in the vasa recta (VR) (F). No staining was detected in the control sections (B, E); ×100, A, B, D, E; ×400, C; ×1000, F.

second mutation not detected; (24) and unpublished data]. While fibrocystin was detected in the normal control, no products were seen in the ARPKD kidneys (Fig. 1C and data not shown). To show that large molecular weight collecting duct derived protein was present in these samples, an identical filter was probed with an epithelial membrane antigen (EMA) antibody that detects large glycosylated products (Fig. 1C). Together these data provide strong evidence that these mAbs detect a large, membrane bound form of fibrocystin.

Analysis of a range of adult murine tissues (brain, lung, heart, pancreas, testis and liver) showed that the large fibrocystin product was not strongly detected in any other organ, but weak expression of the >450 kDa product, and moderate levels of the ∼220 kDa product, plus a ∼150 kDa protein, was seen in liver (Fig. 1B).

Determining the cellular distribution of fibrocystin

To determine the cellular distribution of fibrocystin, formalin-fixed human tissue of fetal, childhood and adult ages were analyzed with the mAbs FB5 and FB1. Similar results were obtained with both mAbs, and representative images of both antibodies are illustrated. In embryonic human kidney immunohistochemical staining for fibrocystin was localized to branching ureteric ducts and collecting ducts, with weaker staining in the developing nephron (Fig. 2A–C). No staining was detected in the uninduced or condensating mesenchyma. In the infantile kidney the collecting duct stained strongly and signal was also detected in the loops of Henle (Fig. 2D–F). In the adult, staining for fibrocystin was restricted mainly to collecting ducts (Fig. 3A–D) with little signal detected in the cortex (Fig. 3E and F). The pattern of staining was often cytoplasmic, but possible apical plasma membrane signal was also detected (Fig. 3C and D). Analysis of ARPKD kidney from one available sample (R328) with defined *PKHD1* mutations (5895insA and L1407R) (24) showed little staining of the dilated collecting ducts consistent with loss of the protein in the disease tissue (Fig. 3G).

In human liver, fibrocystin was detected in developing and mature intrahepatic bile ducts with faint staining also detected in hepatocytes (Fig. 4A–C). Analysis of three liver samples from ARPKD patients, two with defined *PKHD1* mutations (R895; Q3392X, I222V and R947; C1249W, Q1917R) showed a lack of staining of bile duct epithelium in each case (Fig. 3H and data not shown). Fibrocystin was also detected in other tissues including pancreatic ducts and islets (Fig. 4D–F), the epididymal duct (Fig. 4G) and seminiferous tubules of the testis (Fig. 4H and I) and the adrenal gland (data not shown).

Subcellular localization of fibrocystin in MDCK cells

Recent studies of various forms of PKD have highlighted cilia as a likely functional location of the cystogenic protein. To determine if fibrocystin is also localized to cilia in kidney cells, immunofluorescent staining of MDCK cells was performed. These cells were selected as they are derived from the collecting duct (a site of fibrocystin expression) and known to form long cilia in culture (13). Cells were grown on coverslips and maintained at confluence for between 5–9 days before fixation, to ensure ciliary development. The cells were stained with the fibrocystin antibody FB5 and acetylated α-tubulin, a ciliary marker. Figure 5A–C shows in a low magnification image that most cells express a single cilium. A complete correspondence between the fibrocystin and tubulin staining is observed, showing that fibrocystin is localized to the ciliary axoneme in MDCK cells. At a high magnification in cells at confluence for 9 days, especially long cilia are observed and again the correspondence of the two proteins along the

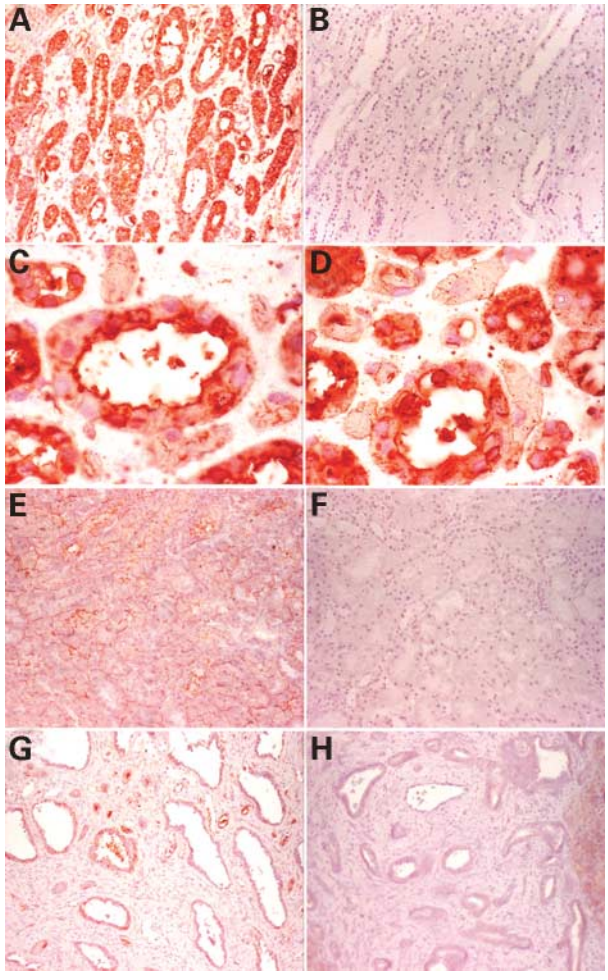

Figure 3. Normal adult renal medulla (**A**–**D**) and cortex (**E**, **F**), detected with the fibrocystin FB5 monoclonal antibody. The staining is mostly confined to the collecting ducts (A, C, D). No staining was detected in the control sections (B, F). At higher magnification apical accentuation of the immunostaining is noticeable (C, D). Analysis of ARPKD kidney (**G**) and liver (**H**) shows no staining of collecting ducts or bile ducts, respectively; ×200, A, B, E–H; ×1000, C, D.

length of the cilia can be observed. In Z-section, individual cilia projecting from the apical surface are stained with tubulin and fibrocystin (Fig. 5D–F, J–L).

DISCUSSION

We describe here the first antibodies to the ARPKD protein, fibrocystin. Detection of the same sized large proteins in human kidney membrane preparations with all four mAbs, identification of the same product in rat and mouse kidney and liver and loss of the products in ARPKD kidney and liver, provide compelling evidence that these antibodies see fibrocystin. The presence of the >450 kDa protein in purified membrane protein and the size similarity to the predicted full-length protein (plus possible N-linked glycosylation), strongly suggests that this product is full-length, membrane-bound, fibrocystin. The structure of the smaller (~220 kDa) product is less clear but its presence in the human kidney and loss in ARPKD renal tissue suggest that it is also cognate to fibrocystin. The intensity of this fragment is somewhat variable in different protein preparations; Figure 1A shows the typical relative abundance of the two species in kidney. In liver the >450 kDa product was also seen, but the ~220 kDa band was often prominent, and an additional ~150 kDa band was usually detected (Fig. 1B). These smaller proteins may represent membrane-bound products of specific splice variants, not encoding parts of the extracellular region. However, the variable intensities of these products in different experiments suggest that the smaller species may be degradation products.

The results described here are unlikely to represent all fibrocystin products as only membrane bound proteins containing the C-terminal tail will be recognized with these antibodies. Analysis of potential alternatively spliced products of *PKHD1* indicate that other shorter and possibly secreted products may be generated that will not be detected with the present reagents. Development of further antibodies recognizing the extracellular part of the protein will be required to characterize the full array of products.

The loss of fibrocystin in ARPKD kidney is consistent with a recessive disease where all protein may be lost. The ARPKD tissues that were analyzed were mainly from severely affected cases and in each case one (at least) of the mutant alleles contained a missense mutation (see Results). The loss of all protein detected with the C-terminal antibody suggests that the mutant fibrocystin in these cases is destabilized and rapidly degraded. It would be interesting to analyze tissue from less severely affected patients where we might expect some residual fibrocystin.

The cellular distribution of the protein to the ureteric bud and collecting ducts of the developing kidney and to distal structures in the adult is consistent with the pattern of tubular dilation characteristic of ARPKD (20). The staining of intrahepatic bile ducts and pancreatic ducts are also consistent with sites of ARPKD disease and mRNA expression (22). Other areas of staining, such as hepatocytes and testicular structures, are not recognized sites of disease and will require further studies to confirm. It is difficult from immunohistochemical staining to determine the subcellular localization of fibrocystin, although the pattern of significant cytoplasmic signal is reminiscent of that seen with the ADPKD protein, polycystin-1. As in that case, this may reflect protein that is being processed for ciliary and/or plasma membrane localization, or recycling from the surface of the cell (33,34). In some high-resolution images of ductal structures, apical membrane staining of fibrocystin is suggested (Figs 3C and 4E and I).

To better determine the subcellular localization of fibrocystin we have analyzed cultured MDCK cells by immunofluorescence. This analysis showed clear staining of the ciliary axonome in confocal images focused above the surface of the cell. However, some cystoplasmic signal was also seen. It remains to be determined if the ciliary localization is the only functional site of fibrocystin or if apical plasma membrane or internal membrane localizations are important for normal function. Furthermore, only membrane bound products are recognized by these reagents and other secreted products may exist. The ciliary fibrocystin staining further emphasizes the link between PKD and the cilia with a total of seven human or animal diseases now showing this connection (6–12,15). It has

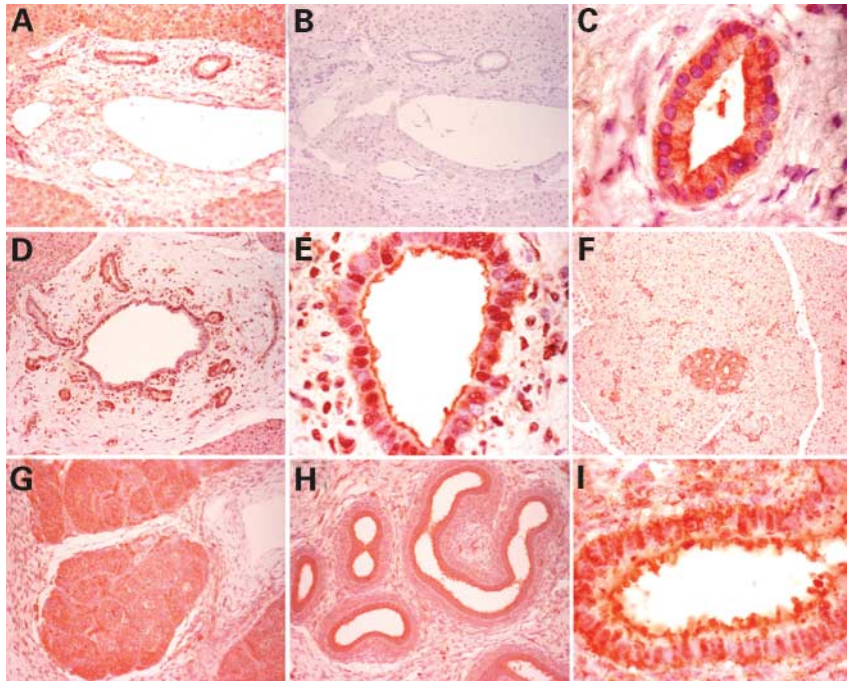

Figure 4. Immunohistochemical staining for fibrocystin in adult liver (**A**–**C**), 3-year-old pancreas (**D**–**F**), and 30 week embryonic testes (**G**) and epididymis (**H**, **I**) using the FB5 monoclonal antibody. Immunostaining is detected in the bile ducts (A, C), pancreatic ducts (D, E), pancreatic islets (F), seminiferous tubules of the testis (G) and epididymal duct (H, I). Immunostaining is mainly detected in the epithelial cells lining the tubular structures, in the pancreatic islets and in the seminiferous tubules. Weaker immunostaining is also noted in the hepatocytes. No staining was detected in the control section (B); ×200, A, B, D, F–H; ×1000 C, E, I.

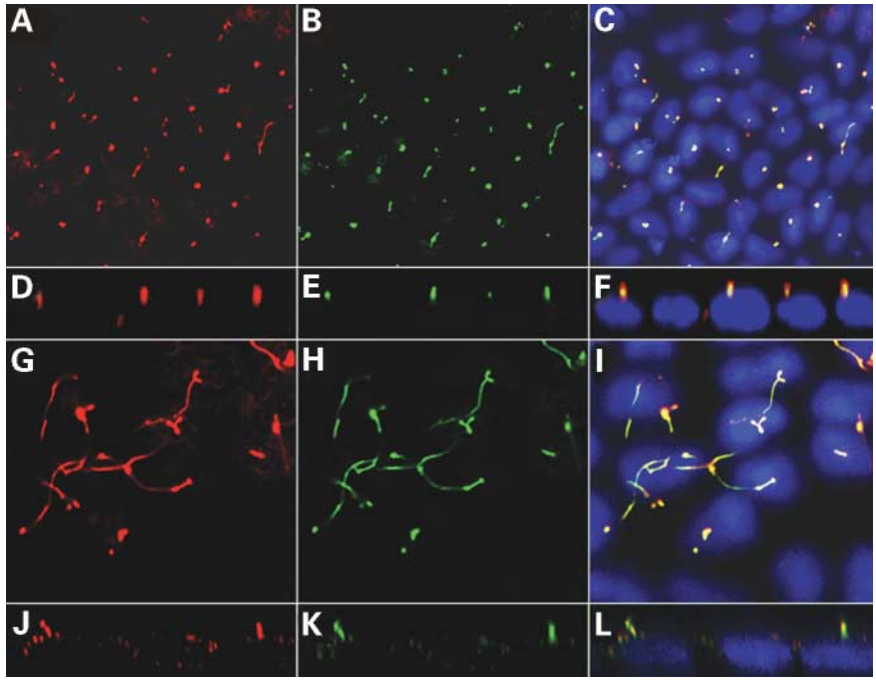

Figure 5. Immunofluorescence of confluent MDCK cells with: (**A**, **D**, **G**, **J**) the ciliary protein, acetylated α-tubulin (red); (**B**, **E**, **H**, **K**) the fibrocystin mAB FB5 (green) and (**C**, **F**, **I**, **L**) both antibodies, plus DAPI staining of the nuclei. Confocal images are focused above the apical surface of the cell and co-localization shows that fibrocystin is expressed in the ciliary axonome. Analysis of longer MDCK cilia (G–I) showed fibrocystin along the length of the cilia (green), localized with acetylated α-tubulin (red). In a 90 nm *Z*-section (D–F, J–L) individual cilia are seen projecting from the apical surface and stained for both proteins.

been suggested that polycystin-1 and -2 are associated with the Ca^{2+} influx induced by movement of cilia and indicating a mechanosensory function (12). It is not clear if fibrocystin is also involved in this mechanosensory role of cilia, but it is interesting to note that the structure of fibrocystin, with a large extracellular region containing multiple copies of an immunoglobulin-like fold, is somewhat reminiscent of the extracellular part of polycystin-1 (24,35). Other possible roles for cilia in cyst formation are as tubule size sensors (36). These may act as important checkpoints in tubule maturation that when defective can lead to the tubule dilatation that characterizes the kidney and liver disease in ARPKD. Related studies have shown ciliary abnormalities in the PCK model of ARPKD indicating that (similar to the *orpk* model of PKD) loss of fibrocystin can influence ciliary structure as well as function (37). Further study will be required to see where fibrocystin fits into the ciliary, PKD puzzle, but the localization data and reagents described here should provide a stimulus to answer those questions.

MATERIALS AND METHODS

Monoclonal antibody production

The *PKHD1* fragment was amplified and cloned into a modified pET-43a$^+$ (Novagen) vector with a tobacco etch virus (TEV) protease site between the NusA ORF and the *PKHD1* region. The NusA-fibrocystin fusion protein was produced in *E. coli* AD494 DE3, purified by cobalt affinity chromatography (TALON resin, Clontech), cleaved using recombinant TEV protease and the fibrocystin portion purified by ion exchange chromatography using a MilliQ column in 4 M urea, 20 mM Tris pH 8.0 and a gradient of NaCl from 0 to 1 M. BALB/c ByJ mice were immunized with the purified fibrocystin molecule and monoclonal antibodies generated (38). Isotypes of the fibrocystin mAbs are: FB1, FB2, FB8, IgMκ; FB5, IgG2aκ.

Membrane protein isolation and western blotting

The membrane protein was prepared largely as previously published (39). One gram of microtome sliced tissue was homogenized for 3 min in 1 ml of buffer 1 (10 mM Tris–HCl pH 7.4, 0.25 M sucrose, and 0.2 mM $CaCl_2$). Five milliliters of buffer 2 (10 mM Tris–HCl pH 7.4, 0.25 M sucrose, and 1 mM EDTA) were added and the mixture centrifuged (4000*g*, 5 min) to remove nuclei and debris. The supernatant was overlayed onto a 35% (w/v) sucrose cushion, centrifuged (30 000*g*, 30 min, 4°C), the interface collected and diluted with buffer 3 (10 mM Tris–HCl pH 7.4, 0.25 M sucrose) and pelleted (100 000*g*, 45 min, 4°C). The membrane protein was dissolved in 0.2–0.5 ml buffer 3 and stored at −80°C. All solutions contained the complete proteinase inhibitor cocktail (Roche Molecular Biochemicals).

For western blotting, the membrane protein was mixed with 2 µl, 1 M DTT and sample buffer (Invitrogen), incubated at 70°C for 10 min, loaded on a 3–8% Tris–acetate NuPAGE gel (Invitrogen), electrophoresed (30 V for 8 h), and transferred to the Invitrolon PVDF membrane (Invitrogen) using the NuPAGE transfer buffer (Novex) at 30 V for 2 h. The membrane was incubated in blocking solution (1 × PBS, 5% milk powder, and 0.05% Tween-20) for 2 h at room temperature, or overnight at 4°C, and probed with neat hybridoma supernatant. The membrane was washed three times in 1 × PBS and 0.05% Tween-20, incubated in the blocking solution at room temperature (10 min) and detected with an isotype specific horseradish peroxidase conjugated goat anti-mouse antibody (Southern Biotechnology Associates Inc.; 1 : 200 dilution) in blocking solution for 1 h. The membrane was subsequently washed as above and the peroxidase detected using the chemiluminescent substrate, Luminol Reagent (Santa Cruz Biotechnology) and exposed to Biomax film (Kodak). The MANCHO3 8A4 utrophin mAb (32) and an EMA antibody (M0613, Dako) were employed as controls.

Immunohistochemistry

Fetal (26–36 weeks), childhood (3 months to 4 years of age) and adult human tissues for immunohistochemistry were obtained at autopsy or at surgery (from normal tissues resected for renal carcinoma or hepatoma). ARPKD tissues were obtained from surgeries or biopsies. The tissues were fixed in 10% formaldehyde and embedded in paraffin. Tissue sections (5 µm) were deparaffinized in xylene, rehydrated in graded ethanol series, and rinsed in tap water. Endogenous peroxidase activity was blocked using 50% methanol/1.5% H_2O_2. After sections were rinsed in tap water, they were microwaved for 2 min in 10 mM citrate buffer (pH 6.0), allowed to cool for 20 min, and again rinsed in tap water. Sections were treated with 10% normal goat serum in PBS for 20 min, incubated at room temperature with the primary antibody at an appropriate dilution for 45 min, rinsed in PBS, and treated with biotinylated anti-mouse antibodies (BioGenex Inc., San Ramon, CA, USA) for 20 min, followed by peroxidase-conjugated streptavidin (BioGenex) for 20 min at room temperature. Sections were developed in AEC solution (BioGenex). Counterstaining was carried out with hematoxylin, and coverslips were attached using aqueous mounting media.

Immunofluorescence

MDCK cells were grown on collagen-coated coverslips and kept at confluence for at least 5 days before analysis. The cells were washed briefly in PBS (pH 7.1), fixed in methanol at −20°C for 3–5 min and washed three times in PBS and 0.5% Triton-X. The coverslips were incubated for 45 min in 1% BSA, 5% goat serum and 0.5% Triton-X before incubation with the primary antibody for 2 h at room temperature. After washing three times in PBS they were treated with secondary antibody in 1% BSA for 1 h at room temperature and washed three times in PBS before mounting. The acetylated α-tubulin antibody (Sigma, T6793) was used to detect cilia. Nuclei were counter-stained with DAPI. Microscopy was performed with a Zeiss LSM 510 confocal microscopy with a 100× Pan-Apochromat 1.4 nm oil objective. Images were taken above the apical surface of the cell to illustrate ciliary staining. A single pixel vertical slice (90 nm) was made through assembled optical *X*–*Y* sections of the cell layer for the *Z*-sections (Fig. 5D–F, J–L).

ACKNOWLEDGEMENTS

We thank L.A. Cummins and T.G. Beito (Mayo Monoclonal Antibody Core Facility), J. Tarara (Optical Morphology Core Facility), S. Rossetti for mutation analysis and G.E. Morris for the utrophin mAb. This work was supported by NIDDK grants (DK 59597 and DK 44863), the Polycystic Kidney Disease Foundation and the Mayo Foundation.

REFERENCES

1. Carone, F.A., Bacallao, R. and Kanwar, Y.S. (1996) Pathogenesis of polycystic kidney disease: basement membrane and extracellular matrix. In Watson, M.L. and Torres, V.E. (eds), *Polycystic Kidney Disease*. Oxford University Press, Oxford, pp. 111–124.
2. Wilson, P.D. (1996) Pathogenesis of polycystic kidney disease: altered cellular function. In Watson, M.L. and Torres, V.E. (eds), *Polycystic Kidney Disease*. Oxford University Press, Oxford, pp. 125–163.
3. Pazour, G.J., Dickert, B.L., Vucica, Y., Seeley, E.S., Rosenbaum, J.L., Witman, G.B. and Cole, D.G. (2000) *Chlamydomonas IFT*88 and its mouse homologue, polycystic kidney disease gene *Tg*737, are required for assembly of cilia and flagella. *J. Cell Biol.*, **151**, 709–718.
4. Murcia, N.S., Richards, W.G., Yoder, B.K., Mucenski, M.L., Dunlap, J.R. and Woychik, R.P. (2000) The Oak Ridge Polycystic Kidney (orpk) disease gene is required for left–right axis determination. *Development*, **127**, 2347–2355.
5. Mochizuki, T., Saijoh, Y., Tsuchiya, K., Shirayoshi, Y., Takai, S., Taya, C., Yonekawa, H., Yamada, K., Nihei, H., Nakatsuji, N. *et al.* (1998) Cloning of *inv*, a gene that controls left/right asymmetry and kidney development. *Nature*, **395**, 177–181.
6. Watanabe, D., Saijoh, Y., Nonaka, S., Sasaki, G., Ikawa, Y., Yokoyama, T. and Hamada, H. (2003) The left-right determinant Inversin is a component of node monocilia and other 9+0 cilia. *Development*, **130**, 1725–1734.
7. Hou, X., Mrug, M., Yoder, B.K., Lefkowitz, E.J., Kremmidiotis, G., D'Eustachio, P.D., Beier, D.R. and Guay-Woodford, L.M. (2002) Cystin, a novel cilia-associated protein, is disrupted in the cpk mouse model of polycystic kidney disease. *J. Clin. Invest.*, **109**, 533–540.
8. Taulman, P.D., Haycraft, C.J., Balkovetz, D.F. and Yoder, B.K. (2001) Polaris, a protein involved in left-right axis patterning, localizes to basal bodies and cilia. *Mol. Biol. Cell.*, **12**, 589–599.
9. Morgan, D., Eley, L., Sayer, J., Strachan, T., Yates, L.M., Craighead, A.S. and Goodship, J.A. (2002) Expression analyses and interaction with the anaphase promoting complex protein Apc2 suggest a role for inversin in primary cilia and involvement in the cell cycle. *Hum. Mol. Genet.*, **11**, 3345–3350.
10. Lin, F., Hiesberger, T., Cordes, K., Sinclair, A.M., Goldstein, L.S., Somlo, S. and Igarashi, P. (2003) Kidney-specific inactivation of the KIF3A subunit of kinesin-II inhibits renal ciliogenesis and produces polycystic kidney disease. *Proc. Natl Acad. Sci. USA*, **100**, 5286–5291.
11. Yoder, B.K., Hou, X. and Guay-Woodford, L.M. (2002) The polycystic kidney disease proteins, polycystin-1, polycystin-2, polaris, and cystin, are co-localized in renal cilia. *J. Am. Soc. Nephrol.*, **13**, 2508–2516.
12. Nauli, S.M., Alenghat, F.J., Luo, Y., Williams, E., Vassilev, P., Li, X., Elia, A.E., Lu, W., Brown, E.M., Quinn, S.J. *et al.* (2003) Polycystins 1 and 2 mediate mechanosensation in the primary cilium of kidney cells. *Nat. Genet.*, **33**, 129–137.
13. Praetorius, H.A. and Spring, K.R. (2001) Bending the MDCK cell primary cilium increases intracellular calcium. *J. Membr. Biol.*, **184**, 71–79.
14. Pennekamp, P., Karcher, C., Fischer, A., Schweickert, A., Skryabin, B., Horst, J., Blum, M. and Dworniczak, B. (2002) The ion channel polycystin-2 is required for left–right axis determination in mice. *Curr. Biol.*, **12**, 938–943.
15. Pazour, G.J., San Agustin, J.T., Follit, J.A., Rosenbaum, J.L. and Witman, G.B. (2002) Polycystin-2 localizes to kidney cilia and the ciliary level is elevated in orpk mice with polycystic kidney disease. *Curr. Biol.*, **12**, R378–380.
16. Guay-Woodford, L.M. (1996) Autosomal recessive polycystic kidney disease: clinical and genetic profiles. In Watson, M.L. and Torres,V.E. (eds), *Polycystic Kidney Disease*. Oxford University Press, New York, pp. 237–266.
17. Zerres, K., Mücher, G., Becker, J., Steinkamm, C., Rudnik-Schöneborn, S., Heikkilä,P., Rapola, J., Salonen, R., Germino, G.G., Onuchic, L. *et al.* (1998) Prenatal diagnosis of autosomal recessive polycystic kidney disease (ARPKD): molecular genetics, clinical experience, and fetal morphology. *Am. J. Med. Genet.*, **76**, 137–144.
18. MacRae Dell, K.M. and Avner, E.D. (2001) Autosomal recessive polycystic kidney disease. In *GeneReviews; Genetic Disease Online Reviews at GeneTests-GeneClinics*. University of Washington, Seattle, WA.
19. Roy, S., Dillon, M.J., Trompeter, R.S. and Barratt, T.M. (1997) Autosomal recessive polycystic kidney disease: long-term outcome of neonatal survivors. *Pediatr. Nephrol.*, **11**, 302–306.
20. Osathanondh, V. and Potter, E.L. (1964) Pathogenesis of polycystic kidneys. Type 1 due to hyperplasia of interstitial portions of the collecting tubules. *Arch. Pathol.*, **77**, 466–473.
21. Blyth, H. and Ockenden, B.G. (1971) Polycystic disease of kidneys and liver presenting in childhood. *J. Med. Genet.*, **8**, 257–284.
22. Jorgensen, M.J. (1977) The ductal plate malformation: a study of the intrahepatic bile duct lesion in infantile polycystic disease and congenital hepatic fibrosis. *Acta. Pathol. Microbiol. Scand. Suppl.*, 1–87.
23. Zerres, K., Mücher, G., Bachner, L., Deschennes, G., Eggermann, T., Kääriäinen, H., Knapp, M., Lennert, T., Misselwitz, J., von Mühlendahl, K.E. *et al.* (1994) Mapping of the gene for autosomal recessive polycystic kidney disease (ARPKD) to chromosome 6p21-cen. *Nat. Genet.*, **7**, 429–432.
24. Ward, C.J., Hogan, M.C., Rossetti, S., Walker, D., Sneddon, T., Wang, X., Kubly, V., Cunningham, J.M., Bacallao, R., Ishibashi, M. *et al.* (2002) The gene mutated in autosomal recessive polycystic kidney disease encodes a large, receptor-like protein. *Nat. Genet.*, **30**, 259–269.
25. Onuchic, L.F., Furu, L., Nagasawa, Y., Hou, X., Eggermann, T., Ren, Z., Bergmann, C., Senderek, J., Esquivel, E., Zeltner, R. *et al.* (2002) *PKHD1*, the polycystic kidney and hepatic disease 1 gene, encodes a novel large protein containing multiple immunoglobulin-like plexin-transcription-factor domains and parallel beta-helix 1 repeats. *Am. J. Hum. Genet.*, **70**, 1305–1317.
26. Nagasawa, Y., Matthiesen, S., Onuchic, L.F., Hou, X., Bergmann, C., Esquivel, E., Senderek, J., Ren, Z., Zeltner, R., Furu, L. *et al.* (2002) Identification and characterization of *Pkhd1*, the mouse orthologue of the human ARPKD gene. *J. Am. Soc. Nephrol.*, **13**, 2246–2258.
27. Xiong, H., Chen, Y., Yi, Y., Tsuchiya, K., Moeckel, G., Cheung, J., Liang, D., Tham, K., Xu, X., Chen, X.Z. *et al.* (2002) A novel gene encoding a TIG multiple domain protein is a positional candidate for autosomal recessive polycystic kidney disease. *Genomics*, **80**, 96–104.
28. Bork, P., Doerks, T., Springer, T.A. and Snel, B. (1999) Domains in plexins: links to integrins and transcription factors. *Trends Biochem. Sci.*, **24**, 261–263.
29. Hogan, M.C., Griffin, M.D., Rossetti, S., Torres, V.E., Ward, C.J. and Harris, P.C. (2003) *PKHDL1*, a homolog of the autosomal recessive polycystic kidney disease gene, encodes a receptor with inducible T lymphocyte expression. *Hum. Mol. Genet.*, **12**, 685–689.
30. Park, M., Dean, M., Kaul, K., Braun, M.J., Gonda, M.A. and Van de Woude, G. (1987) Sequence of MET protooncogene cDNA has features characteristic of the tyrosine kinase family of growth-factor receptors. *Proc. Natl Acad. Sci. USA*, **84**, 6379–6383.
31. Tamagnone, L., Artigiani, S., Chen, H., He, Z., Ming, G.I., Song, H., Chedotal, A., Winberg, M.L., Goodman, C.S., Poo, M. *et al.* (1999) Plexins are a large family of receptors for transmembrane, secreted, and GPI-anchored semaphorins in vertebrates. *Cell*, **99**, 71–80.
32. Nguyen, T.M., Ellis, J.M., Love, D.R., Davies, K.E., Gatter, K.C., Dickson, G. and Morris, G.E. (1991) Localization of the DMDL gene-encoded dystrophin-related protein using a panel of nineteen monoclonal antibodies: presence at neuromuscular junctions, in the sarcolemma of dystrophic skeletal muscle, in vascular and other smooth muscles, and in proliferating brain cell lines. *J. Cell. Biol.*, **115**, 1695–1700.
33. Ward, C.J., Turley, H., Ong, A.C.M., Comley, M., Biddolph, S., Chetty, R., Ratcliffe, P.J., Gatter, K. and Harris, P.C. (1996) Polycystin, the polycystic kidney disease 1 protein, is expressed by epithelial cells in fetal, adult and polycystic kidney. *Proc. Natl Acad. Sci. USA*, **93**, 1524–1528.
34. Ong, A.C. (2000) Polycystin expression in the kidney and other tissues: complexity, consensus and controversy. *Exp. Nephrol.*, **8**, 208–214.
35. Hughes, J., Ward, C.J., Peral, B., Aspinwall, R., Clark, K., San Millán, J.L., Gamble, V. and Harris, P.C. (1995) The polycystic kidney disease 1 (*PKD1*) gene encodes a novel protein with multiple cell recognition domains. *Nat. Genet.*, **10**, 151–160.

36. Lubarsky, B. and Krasnow, M.A. (2003) Tube morphogenesis: making and shaping biological tubes. *Cell*, **112**, 19–28.
37. Masyuk, T.V., Huang, B.Q., Ward, C.J., Masyuk, A.I., Yuan, D., Splinter, P.L., Punyashthiti, R., Ritman, E.L., Torres, V.E., Harris, P.C. *et al.* (2003) Defects in cholangiocyte fibrocystin expression and ciliary structure in the PCK rat. *Gastroenterology*, in press.
38. de StGroth, S.F. and Scheidegger, D. (1980) Production of monoclonal antibodies: strategy and tactics. *J. Immunol. Meth.*, **35**, 1–21.
39. Cai, Y., Maeda, Y., Cedzich, A., Torres, V.E., Wu, G., Hayashi, T., Mochizuki, T., Park, J.H., Witzgall, R. and Somlo, S. (1999) Identification and characterization of polycystin-2, the PKD2 gene product. *J. Biol. Chem.*, **274**, 28557–28565.